d = particle diameter, L

d_{50} = median particle diameter; 50% wt of particles are larger than d_{50}, L

f = friction factor, dimensionless

h = channel height, L

k = von Karman constant

K_j = parameter; $w_j/\zeta u_*$, dimensionless

K_j' = parameter; $w_j/\xi u_*$, dimensionless

R = pipe inside radius, L

$\overline{U}$ = mean flow velocity, LT^{-1}

u_* = friction velocity, $\overline{U}(f/2)^{1/2}$, LT^{-1}

$\mathbf{u}_j$ = particle velocity vector

v_i = relative particle concentration; defined by Equation (20), dimensionless

v_y = liquid velocity in the vertical direction y, LT^{-1}

$\mathbf{v}$ = liquid velocity vector

w_i = particle settling velocity corresponding to d_i, LT^{-1}

y' = reduced vertical coordinate, y/R, dimensionless

$\mathbf{y}$ = unit vector

Greek Letters

ϵ = diffusivity, L^2T^{-1}

ϵ_j = particle diffusivity, L_2T^{-1}

ϵ_l = diffusivity of liquid

$\overline{\epsilon}$ = mean rate of energy dissipation per unit mass of fluid; $2f\overline{U}^3/D$, L^2T^{-3}

ζ = dimensionless diffusivity in pipe flow; ϵ/Ru_*, dimensionless

η = Kolmogorov microscale; $(\nu^3/\overline{\epsilon})^{1/4}$, L

ν = fluid kinematic viscosity, L^2T^{-1}

ξ = dimensionless diffusivity in closed channel flow; ϵ/hu_*, dimensionless

LITERATURE CITED

Abramowitz, M., and I. A. Stegun, ed., *Handbook of Mathematical Functions*, National Bureau of Standards, Applied Math Series 55 (June, 1965).

Barnard, B. J. S., and A. M. Binnie, "The Vertical Diffusivity and Mean Velocity of Particles in a Horizontal Water Pipe," *J. Fluid Mech.*, **15**, 35 (1963).

Batchelor, G. K., "The Motion of Small Particles in Turbulent Flow," *Proceedings, Second Australasian Conference on Hydraulics and Fluid Mechanics,* The University of Auckland, New Zealand, pp. 19-41 (1966).

Binnie, A. M., and O. M. Phillips, "The Mean Velocity of Slightly Buoyant and Heavy Particles in Turbulent Flow in a Pipe," *J. Fluid Mech.*, **4**, 87 (1958).

Durand, R., and E. Condolios, "The Hydraulic Transport of Coal and Solid Materials in Pipes," Paper IV, *Proceedings of Colloquium on the Hydraulic Transport of Coal,* held by the National Coal Board in London (Nov. 5-6, 1952).

Elder, J. W., "The Dispersion of Marked Fluid in Turbulent Shear Flow," *J. Fluid Mech.*, **5**, 544-560 (1959).

Howard, N. M., "Experimental Measurements of Particle Motion in a Turbulent Pipe Flow," PhD thesis, Univ. Ill., Urbana (1974).

Hunt, J. N., "The Turbulent Transport of Suspended Sediment in Open Channels," *Royal Society of London, Proc., Series A*, **224**, No. 1158, 322-335 (1954).

———, "On the Turbulent Transport of a Heterogeneous Sediment," *Quarterly J. Mechanics and Applied Math.*, **22**, Part 2, 235-246 (1969).

Ismail, H. M., "Turbulent Transfer Mechanism and Suspended Sediment in Closed Channels," *Trans. Am. Soc. Civil Engrs.*, **117**, 409-446 (1952).

Kada, H., and T. J. Hanratty, "Effects of Solids on Turbulence in a Fluid," *AIChE J.*, **6**, No. 4, 624-630 (1960).

Meek, C. C., and B. G. Jones, "Studies of the Behavior of Heavy Particles in a Turbulent Fluid Flow," *J. Atmospheric Sci.*, **30**, No. 2, 239-244 (1973).

O'Brien, M. P., "Review of the Theory of Turbulent Flow and its Relations to Sediment Transport," *Trans. Am. Geophysical Union*, **14**, 487-491 (1933).

Rouse, H., "Modern Conceptions of the Mechanics of Fluid Turbulence," *Trans. Am. Soc. Civil Engrs.*, **102**, 463-505; Discussion, 506-543 (1937).

Sharp, M. E., and I. C. O'Neill, "Lateral Diffusion of Large Particles in Turbulent Pipe Flow," *J. Fluid Mech.*, **45**, Part 3, 575-584 (1971).

Snyder, W. H., and J. L. Lumley, "Some Measurements of Particle Velocity Autocorrelation Functions in a Turbulent Flow," *ibid.*, **48**, Part 1, 41-71 (1971).

Soo, S. L., and S. K. Tung, "Pipe Flow of Suspensions in Turbulent Fluid-Electrostatic and Gravity Effects," *Appl. Scientific Res.*, **40**, No. 2-3, 83-97 (1971).

Manuscript received November 3, 1976; revision received March 7, and accepted March 9, 1977.

Electrochemical Extraction of Copper From Scrap Steel

DER-TAU CHIN

Electrochemistry Department
Research Laboratories
General Motors Corporation
Warren, Michigan 48090

A packed-bed electrochemical method is presented for the removal of copper from scrap steel. The method is based on the principle that at certain potentials, steel can be passivated in a suitable electrolyte, whereas copper dissolves anodically. A rotating hemispherical electrode was used to determine the polarization curves of copper and mild steel in various electrolytes. Extraction tests were carried out with an electrochemical cell composed of a cathodic carbon packed bed and an anodic bed packed with synthesized steel scrap.

SCOPE

Disposal of ferrous solid waste is a national problem. Although total annual steel produced and steel scrapped have reached a steady state in the United States, steel scrap represents only 50% of the raw material for the production of iron and steel. The amount of obsolete scrap not recycled was over 37 million tons in 1970 (Albrecht and McDermott, 1973). One of the major technical obstacles

---

Der-Tau Chin is at Clarkson College of Technology, Potsdam, New York 13676.

to increased use of steel scrap is copper contamination.

Copper impurity has an undesirable effect on steel properties, such as hot shortness during rolling. The maximum copper content specified for high quality steel is 0.1%. The copper content in average No. 2 bundle scrap is 0.5% (Battelle Memorial Institute, 1960). The copper content in other scrap ranges from 0.4% in steel cans to 29% in room air conditioners (Institute of Scrap Iron and Steel, Inc., 1972). The potentially recoverable copper in steel scrap amounts to 210 million kg annually.

So far, there is no suitable method which can economically reduce the copper content of scrap steel to less than 0.1%. The magnetic separator is capable of reducing the copper content of shredded automobile scrap to about 0.3% (Bureau of Mines, 1967). A method based upon hydrometallurgical leaching has been discussed by Oden, Adams, and Fugate (1972). These authors were able to remove only half of the copper in the scrap because of insufficient circulation of leaching solution.

This paper describes a study of the electrochemical extraction of copper from a synthesized steel scrap. The method is based upon the principle that at certain anodic potentials, steel can be passivated in a suitable electrolyte, whereas copper will dissolve anodically. A rotating hemispherical electrode was used to measure the steady state polarization behavior of copper and mild steel in various electrolytes. Extraction tests were subsequently carried out in a flow through, packed-bed electrochemical cell.

CONCLUSIONS AND SIGNIFICANCE

A packed-bed electrochemical method is presented for the removal of copper from scrap steel. The polarization of copper and mild steel in ammoniacal sulfate, ammoniacal carbonate, pyrophosphate, and alkaline cyanide solutions was measured with a rotating hemispherical electrode to determine the potential ranges where steel could be passivated and copper would dissolve anodically into the electrolyte. Extraction tests with these electrolytes were subsequently carried out in an electrochemical cell composed of a cathodic carbon bed and an anodic bed filled with synthesized scrap steel. Excellent separation was achieved with alkaline cyanide solution. The copper content in the scrap was reduced to less than 0.06%. This is a level which has not been attained by any other physical separation method except by careful hand picking. Power consumption for the electrolysis ranged from 0 to 0.49 W·h/g of copper removed, depending upon the current density.

Iron and steel are the primary construction materials. In the United States alone, over 100 million tons are produced each year. At various stages of processing or use, they lose their utilization values and are discarded as solid wastes. The problem of ferrous solid wastes is particularly difficult to handle because of their nonuniform sizes and compositions and because of a stringent quality requirement for reuse in industrial and consumer products. Although ferrous scraps have accounted for 50% of the total raw ferrous charge for the domestic production of iron and steel, the amount not recycled is well over 30 million tons annually. A rough estimate indicates that there have been a total accumulation of 800 million tons of ferrous scraps in the United States in the past three decades. These unrecycled scraps are scattered over the country in open areas, landfills, automobile graveyards, backyards, etc. Their impact on our environment and landscape is profound and incalculable.

Ferrous scrap comes from three basic sources: home or mill revert scrap, which is generated during the production of iron and steel; prompt industrial scrap, which is generated during the fabrication of mill products into consumer and industrial products by the metal working industries; and obsolete scrap, which is generated by society's discards of steel products ranging from junked automobiles and home appliances to steel cans. Scrap quality is an extremely important factor for the recycling of iron and steel scrap. The domestic iron and steel industry has traditionally preferred iron ore as a ferrous raw material because of its known chemistry, consistent size, shape, and quality. Home scrap is consumed within the plant in which it is originated. Prompt industrial scrap also flows smoothly into the ferrous recycle system owing to its known composition and quality. However, the obsolete scrap, because of its heterogeneous sources, unknown quality, and contamination, presents a difficult problem for recycling.

The major technical obstacle for increased use of obsolete scrap is copper contamination. Although copper improves the resistance of steel to atmospheric corrosion, its content must not exceed the solid solubility limit of 0.2% to avoid hot shortness during rolling and undesirable surface for finished products. The maximum copper contamination that is allowable depends upon the steel quality for specific applications:

Low quality steel	Maximum 0.5% copper
Average quality	0.3%
High quality	0.1%
Deep drawing quality	0.05%

By comparison, the copper content in No. 2 bundle scrap averages from 0.48 to 0.58%. In other obsolete scraps, it varies from 0.4% in steel cans to 29% in room air conditioners as shown in Table 1. It should be noted that the figures given in the table refer to heterogeneous mixtures. Copper and steel in the scrap are not chemically bonded nor fused together as alloys. Copper is present in the form of copper plating, electrical wiring, motor, winding, cooling coil, radiator, etc. Table 1 also lists estimated discard rates of various scraps in the United States. It can be calculated that potentially recoverable copper in the scraps amounts to 210 million kg annually.

Copper can be completely separated from these scraps by manual dismantling and careful hand picking. However, the cost of labor is prohibitive, and so far there has not been any other method which can reduce the copper content to less than 0.1%. In the scrap processing industry, junked appliances and automobiles are normally shredded into small pieces with a mechanical shredder. This is followed by passing the shredded scraps through a magnetic separator to separate nonferrous materials from steel. The

Table 1. Sources of Obsolete Scraps and Their Copper Content

	Room air conditioner	Range	Refrigerator	Dishwasher	Washer	Dryer	Auto	Steel cans
Discard rate 10^6 kg/yr	160	300	530	70	500	90	11 600	5 450
Copper %	29	1.0	3.7	2.7	1.6	1.4	1.0	0.4

Source: U.S. Environmental Protection Agency Report EPA-SW-45D-72 (1972).

Bureau of Mines (1967) reported that this procedure could reduce the copper content to about 0.3%. Recently, a hydrometallurgical leaching method has been discussed in the literature (Oden et al., 1973); however, it was able to remove only half of the copper in the scrap because of poor contact with leaching solution.

In this study, a method based upon an electrochemical principle has been investigated. It is well known that at certain anodic potentials steel can be passivated in a suitable electrolyte, whereas copper will dissolve anodically. The separation is achieved in an electrochemical cell composed of two packed columns separated by a cell separator. The anodic column is filled with shredded steel scraps, and the cathodic column is filled with carbon particles. An electrolyte is circulating between the cell and a solution reservoir. When an electric potential is applied across the cell, steel is passivated, and its associated copper dissolves into the electrolyte as copper ions. In theory, copper ions will migrate into the cathodic column, where they are recovered in metallic form. This paper describes the experimental setup and the results of a separation test with four different electrolytes: ammoniacal sulfate, ammoniacal carbonate, pyrophosphate, and alkaline cyanide solutions. These electrolytes are alkaline in nature, and they possess good copper corrosion property. In the absence of chloride ions, iron and steel can be easily passivated in neutral and alkaline solutions. The passive potential range for iron increases with increasing *p*H values. The *p*H of these solutions are greater than 9.5, and, according to the Pourbaix diagram (Pourbaix, 1966), iron may become passivated at the potentials greater than −0.7 V vs. SHE with the formation of a protective magnetic iron oxide film at the surface. On the other hand ammonia, pyrophosphate, and cyanide ions are good complex forming agents for cupric and cuprous ions; they react with copper to form $Cu(NH_4)_4^{2+}$, $Cu(P_2O_7)_2^{6-}$, and $Cu(CN)_3^{2-}$ complex ions, respectively. The anions act as depolarizers and ensure good copper dissolution at anodic potentials.

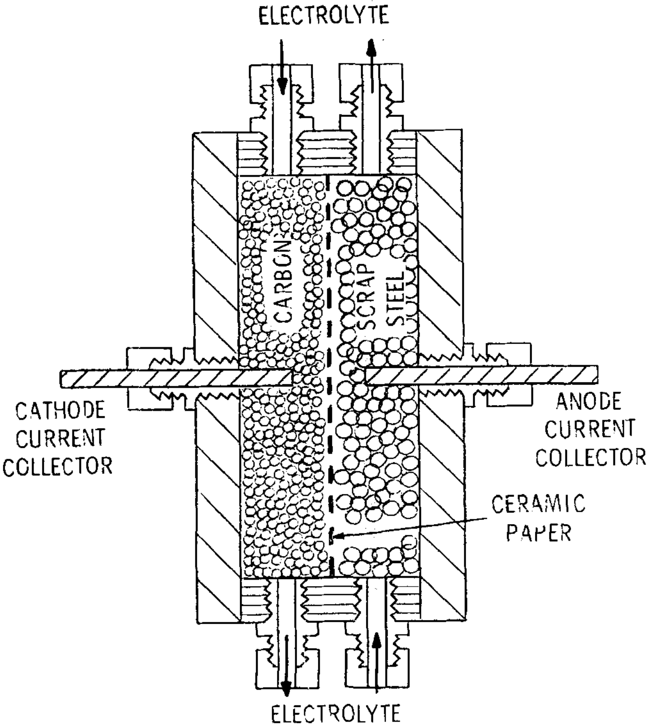

Fig. 1. Packed-bed electrochemical cell for the extraction of copper from scrap steel.

EXPERIMENTAL

Electrolytes

The electrolytes used for this study were: 1M $(NH_4)_2SO_4$ + 1M NH_4OH; 1M $(NH_4)_2CO_3$ + 1M NH_4OH; 0.5M $K_4P_2O_7$ + 0.1M $Na_2C_2O_4$; and 2M NaCN + 0.25M NaOH + 0-1M CuCN. All the solutions were prepared by dissolving the analytical grade chemicals into distilled water without further purification. The temperature of the electrolyte was maintained at 25 ± 2°C.

Steady State Polarization Measurements

To determine the potential range in which the separation might be achieved with the test electrolyte, the steady state polarization of copper and mild steel was measured using a rotating hemispherical electrode. The electrode consisted of a replaceable copper or mild steel hemispherical head mounted on one end of a cylindrical fluorocarbon rod; the other end of the rod was attached to the spindle shaft of a high-speed rotator. The hemispherical heads were 0.635 cm in diameter and had a surface area of 0.63 cm^2 exposed to the electrolyte. Details of the experimental setup are given in previous papers (Chin, 1972; 1974).

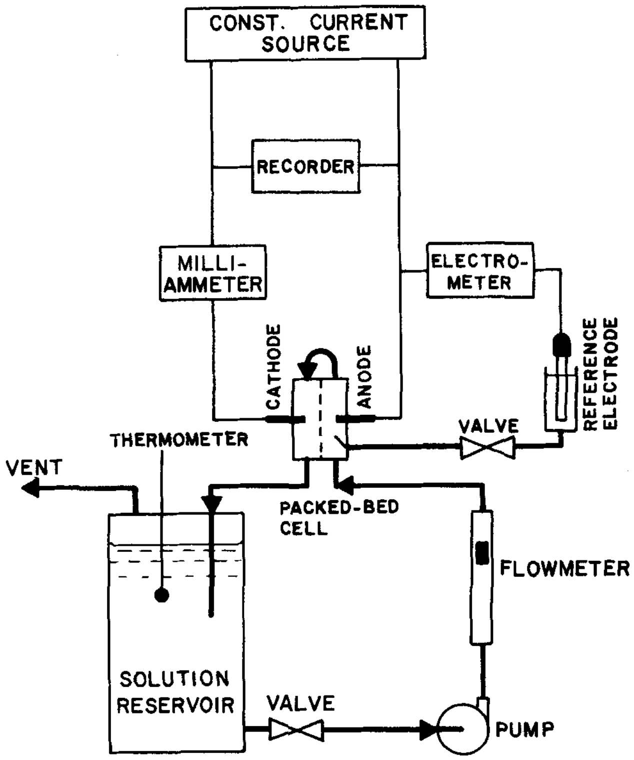

Fig. 2. Schematic diagram for the copper extraction experiment. The thick lines represent the direction of electrolyte flow. The electric connections are indicated by the thin lines.

For each run, the rotating hemispherical electrode was cleaned with methanol and dilute sulfuric acid and rinsed in water. The cleaned electrode was transferred to the cell and installed on the rotator. The polarization was then measured at a fixed speed of rotation using a potentiostat. A saturated calomel electrode was used as the reference electrode for the ammoniacal sulfate and carbonate solutions. For pyrophosphate and alkaline cyanide solutions, a mercury-mercuric oxide electrode was used as the reference electrode.

Packed-Bed Electrodes

Figure 1 shows the construction of the packed-bed electrochemical cell used for the extraction test. It is composed of three sections. The middle section is an acrylic frame. A 0.3 cm thick stainless steel reinforced ceramic paper, located at the middle of the frame, partitioned it into right and left compartments. The other two sections were acrylic compartment covers equipped with replaceable current collectors. The three sections were bolted together to form two rectangular packed columns, each 2.5 cm wide by 5 cm high by 2 cm thick, with a cross-sectional area of 12.5 cm² perpendicular to the direction of flow of electric current. The anodic compartment was equipped with a capillary hole (not shown in the figure) for the measurement of anode potentials.

A synthesized steel scrap composed of 95% steel brads* (A.W.G. #18 by 1.3 cm long), and 5% copper chips† (1 mm diameter by 0.6 cm long) were used to pack the anodic column. The cathodic column was filled with 16 to 20 mesh active carbon particles.** Steel rods, 0.635 cm in diameter and 10 cm long, were used as the current collectors as shown in Figure 1.

The test electrolyte was introduced into the cell at the bottom of the anodic bed. It exited at the top and returned to the cathodic bed via an external U tube. Finally, the electrolyte left the cell at the bottom of the cathodic column. A variable speed, stainless steel pump was used to circulate the electrolyte between the cell and a 2*l* solution reservoir at a rate of 500 ml/min. Figure 2 is a schematic representation of the experimental setup. The direction of electrolyte flow is indicated by the thick lines.

For each run, predetermined amounts of scrap steel (about 0 g) and active carbon (about 12 g) were placed in the cell. A constant current from a potentiostat was applied across the current collectors, and the cell voltage was recorded on a recorder as shown in Figure 2. An electrometer was used to check the potential of the anodic bed to ensure that the bed potential was less than the passive/transpassive transitional potential of mild steel as determined by the rotating hemisphere experiments. After the run, the electrolyte was analyzed chemically to determine the amount of copper and iron dissolved into the solution. The scrap and the active carbon were carefully removed from the packed columns, rinsed in water, and dried at 120°C for 4 hr. They were then weighed to determine the weight gain or loss. The active carbon was subsequently analyzed to determine the amount of iron and copper deposited at the cathode. The remaining copper chips in the scrap were carefully separated from steel using a magnet and weighed to determine the total copper dissolved during the run. The running time varied from 117 hr for a cell current of 20 mA to 7 hr at 200 mA. All the tests were carried out at a temperature of 25 ± 2°C.

RESULTS AND DISCUSSION

Polarization Results

The results of the steady state polarization measurements are given in Figures 3 to 6 for ammoniacal sulfate, pyrophosphate, ammoniacal carbonate, and alkaline cyanide solutions, respectively. For comparison, the mild steel and the copper polarizations in each solution are plotted semilogarithmically in the same figure. Several qualitative conclusions can be made by observing the shape of the curves.

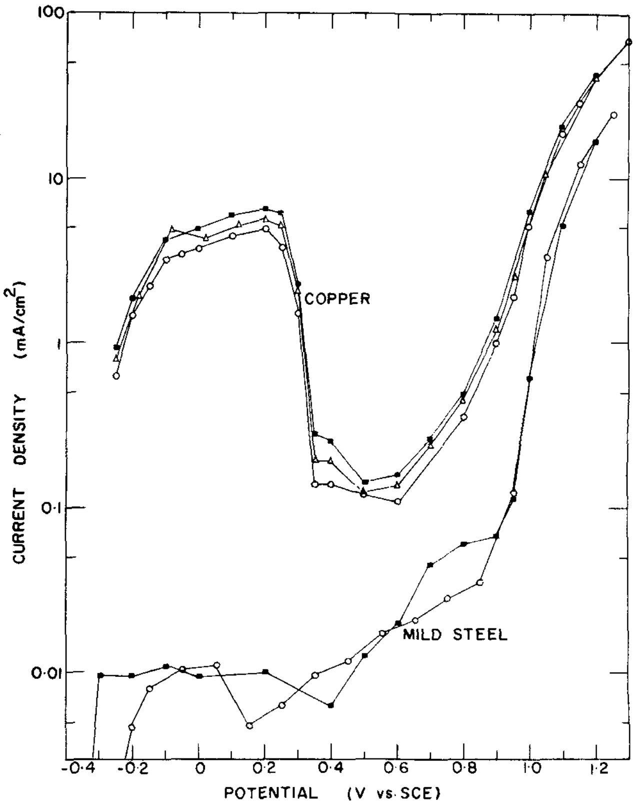

Fig. 3. Polarization of copper and mild steel in mixed $(NH_4)_2SO_4$/NH_4OH electrolyte. Rotation speed: ○, 2 500 rev/min.; ■, 1 600 rev/min; △, 900 rev/min.

1. Copper is passivated in ammoniacal sulfate and pyrophosphate solutions. The shape of the copper curves suggests that the passivation is initiated by the formation of an oxide film. In fact, a black film was observed on the copper electrode when the potential was maintained in the

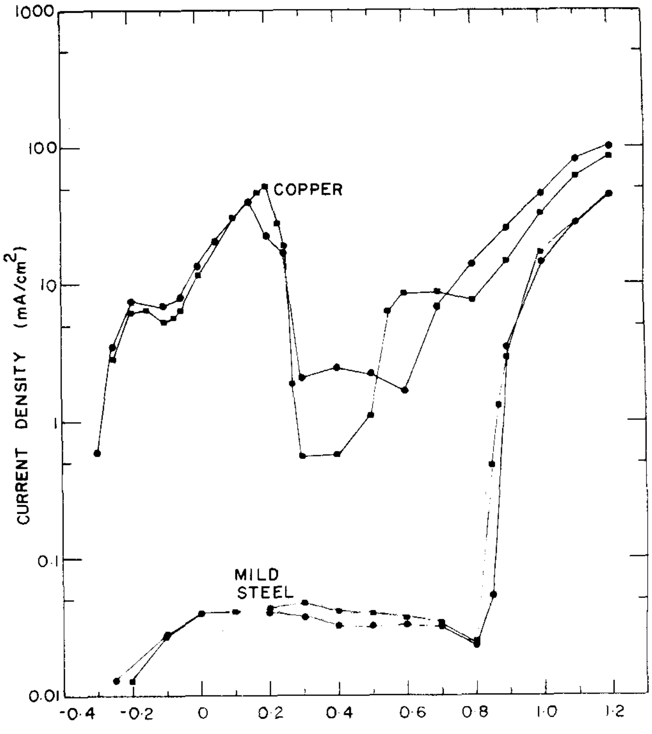

Fig. 4. Polarization of copper and mild steel in mixed $K_4P_2O_7$/$Na_2C_2O_4$ electrolyte. Rotational speed: ●, 3 600 rev/min; ■, 1 600 rev/min.

---

* Composition of steel brad other than iron: carbon, 0.079%; sulfur, 0.026%; manganese, 0.35%; phosphorus, 0.009%; copper, 0.029%.

† Composition of copper chip other than copper: silver, 0.002%; calcium, 0.01%; aluminum, 0.002%; silicon, 0.001%; magnesium, 0.0001%.

** Impurities in the active carbon: copper, 0.003%; iron, 0.3%.

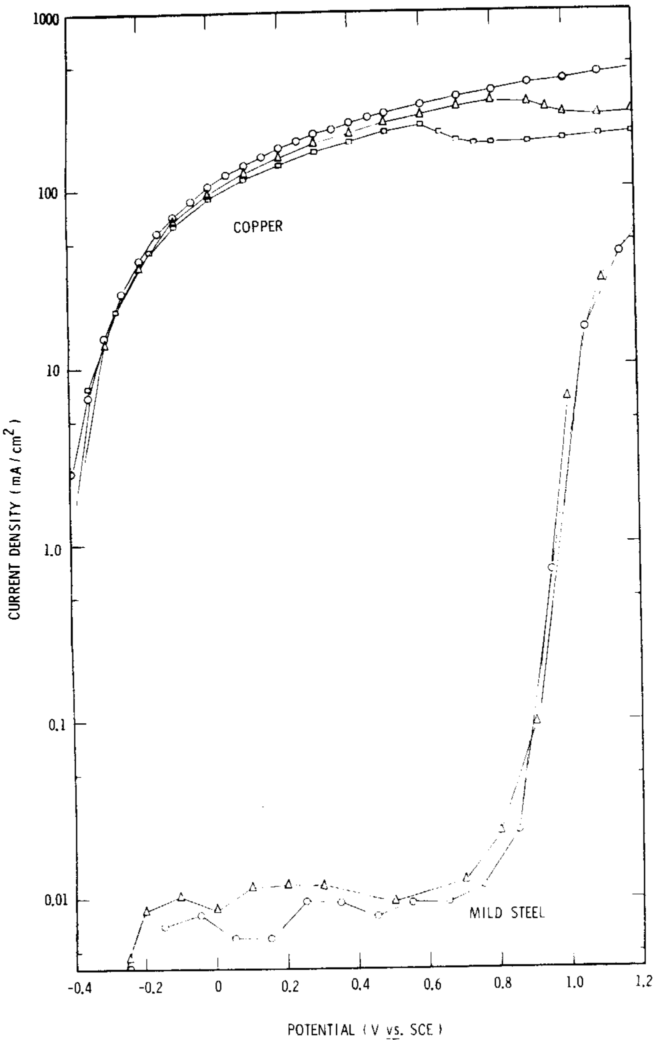

Fig. 5. Polarization of copper and mild steel in mixed $(NH_4)_2CO_3$/NH_4OH electrolyte. Rotational speed: ○, 2 500 rev/min; △, 900 rev/min; □, 400 rev/min.

passive region in these two solutions. This kind of film gives good protection to the anode. One would expect that the anodic corrosion of copper in these two solutions would be poor in the packed-bed operation.

2. Anodic corrosion of copper in ammoniacal carbonate and alkaline cyanide solutions is good. There is a dip in the corrosion current in the polarization curve at high potentials (Figures 5 and 6). The magnitude of the passive current density is high. The transition from the active to the passive state depends on the rotational speed of the hemispherical electrode, the higher the rotational speed, the higher is the critical current density at which the transition from active dissolution to the passive state takes place. This behavior indicates that the passivation is initiated by the formation of a salt layer on the anode surface due to supersaturation of the dissolution product near the electrode (Chin, 1971). The salt layer does not provide protection against anodic corrosion.

3. Mild steel is passivated instantaneously in ammoniacal sulfate, pyrophosphate, and ammoniacal carbonate solutions (Figures 3 to 5); there is no active dissolution region for the mild steel in these three solutions. It would be expected that corrosion of steel would be minimal in these three solutions if the potential of the packed-bed electrode is kept at values less than the transpassive potentials. On the other hand, the polarization curve for mild steel in alkaline cyanide solution (Figure 6) shows an active dissolution region when the electrode potential is

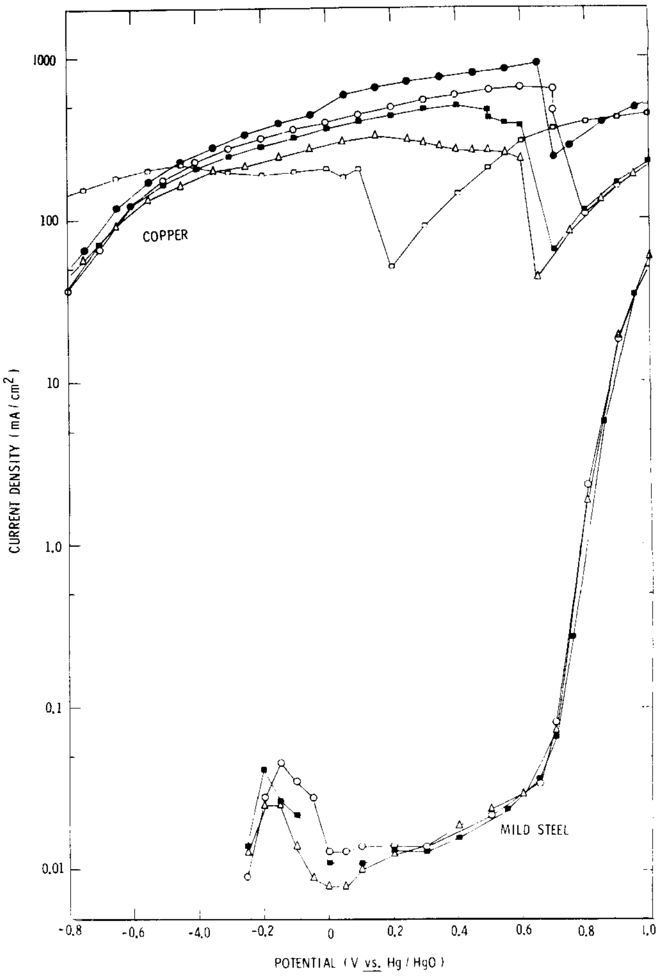

Fig. 6. Polarization of copper and mild steel in mixed NaCN/NaOH electrolyte. Rotational speed: ●, 3 600 rev/min; ○, 2 500 rev/min; ■, 1 600 rev/min; △, 900 rev/min; □, 400 rev/min.

TABLE 2.

(1) Electrolyte	(2) Cell current (mA)	(3) Average cell voltage (V)	(4) Coulombs
1M $(NH_4)_2SO_4$	20	0.39	5 184
+ 1M NH_4OH	40	1.46	9 648
0.5M $K_4P_2O_7$ + 0.1M $Na_2C_2O_4$	40	0.9	9 648
1M $(NH_4)_2CO_3$	20	0.20	8 424
+ 1M NH_4OH	40	0.66	9 216
	100	1.47	15 300
1M $(NH_4)_2CO_3$ + 1M NH_4OH saturated with air	100	2.21	8 640
2M NaCN + 0.25M	20	−0.02	4 752
NaOH	100	0.16	4 320
	200	1.07	5 040
2M NaCN + 0.25M NaOH + 0.5M CuCN	100	1.50	4 860
2M NaCN + 0.25M NaOH + 1M CuCN	50	1.28	4 500

---

[*] Including anode current collectors.
[†] This figure does not include the 0.029% copper originally contained

less than 0 V vs. Hg/HgO. Consequently, some corrosion of steel would be expected during packed-bed operation when the cyanide solution is used as the working electrolyte.

4. The passive/transpassive transitional potential for mild steel is 0.8 V vs. SCE for ammoniacal carbonate solution, 0.8 V vs. Hg/HgO for pyrophosphate solution, and 0.7 V vs. Hg/HgO for alkaline cyanide solution. The transitional potential for ammoniacal sulfate solution is not as sharp; the current density starts to rise slowly at 0.4 V vs. SCE and then increases rapidly with increasing potential at 0.8 V vs. SCE. Since mild steel dissolves into the electrolyte at the transpassive potentials, the potential of the anodic bed during the packed-bed electrode operation should be kept at values lower than the passive/transpassive transitional potentials.

Extraction Tests

The results of the separation tests with the packed-bed electrochemical cell are given in Table 2 for the various electrolytes and test conditions. For each test, percent copper remaining in the scrap, the number of Faradays used per gram-mole of copper removed, and the watt-hours per gram of copper removed are reported in columns (12 to 14), respectively. To determine the extent of separation which might be achieved in a given test, a separation factor is introduced as

$$\text{Separation factor} = \frac{\dfrac{\text{Weight copper removed}}{\text{Total copper in scrap}}}{\dfrac{\text{Weight loss of steel}}{\text{Total steel in scrap}}}$$

Values of the separation factor are reported in column (9). The total amount of steel dissolved in the anodic bed is given in column (8). It should be noted that the weight loss of the cathodic steel current collector was negligibly small. The weight loss of the anodic current collector ranged from 0.3 to 5% of the total steel dissolved, depending upon the magnitude of the cell currents and the type of electrolytes used. There is an offset of about 10% if one tries to calculate a copper balance from columns (6), (7), (10), and (11). This offset is primarily due to loss or evaporation of the electrolyte during the test and to the use of spectrographic analysis of the carbon samples. The values reported for the weight of copper deposited at the cathode bed [column (11)] are semiquantitative estimates calculated from the results of the spectrographic analysis. The actual values are expected to be within one-third to three times the reported values.

Ammoniacal sulfate and pyrophosphate solutions. In these two solutions, the anodic corrosion of copper is poor, as expected from the polarization studies. This is especially true at high current densities, because copper tends to be passivated at high potentials. It can be seen that, at a cell current of 40 mA, the power consumption [column (14)] is almost ten times larger than that at 20 mA. A big advantage of the pyrophosphate solution is that copper can be easily deposited at the cathode; almost all the copper dissolved is recovered at the cathode bed. The separation factors for these two systems are high, ranging from 800 for the pyrophosphate solution to 14 000 for the ammoniacal sulfate solution.

Ammoniacal carbonate solution. The quantity of copper dissolved in ammoniacal carbonate solution decreased rapidly with increasing cell current. This is a surprising result, for copper does not seem to be passivated in this solution, as shown in Figure 5. It was subsequently learned that dissolved oxygen played an important role in the copper dissolution reaction. A test was, therefore, made with air saturated ammoniacal carbonate solution. It can be seen (Table 2) that air substantially increased the copper corrosion; at 100 mA, the number of Faradays per gram-mole of copper dissolved decreased from 4.8 without

RESULTS OF EXTRACTION TESTS WITH THE PACKED BED ELECTROCHEMICAL CELL

(5) and (6) Weight of scrap (g) Steel	Copper	(7) Total copper dissolved (g)	(8) Total steel dissolved* (g)	(9) Separation factor	(10) Copper recovered from electrolyte (g)	(11) Copper deposited at cathode bed (%)	(12) Copper remaining in scrap* (g)	(13) Faradays/g/mole copper dissolved	(14) $W \cdot h/g$ of copper dissolved
56.916	3.006	2.806	0.025	2 125	2.7	0.24	0.35	1.22	0.20
56.938	3.109	2.051	0.017	2 210	2.05	0.005	1.83	3.10	1.91
57.088	3.023	1.106	0.025	835	—	1.17	3.25	5.75	2.18
57.036	3.125	3.120	0	∞	3.0	0.12	0.009	1.78	0.15
57.068	3.191	2.804	0	∞	2.76	0.12	0.67	2.16	0.60
57.168	3.060	2.087	0.010	3 900	2.06	0	1.67	4.83	2.23
57.086	2.869	2.796	0.012	4 590	2.72	0.025	0.13	2.04	1.87
57.082	2.953	2.952	0.809	70.5	3.0	0	0.001	1.06	−0.01
56.835	3.037	3.000	0.158	355	3.1	0	0.06	0.95	0.064
56.882	3.068	3.050	0.090	628	3.1	0	0.03	1.09	0.49
56.805	3.141	2.505	0.047	964	2.2	0	1.11	1.28	0.81
56.896	3.077	0.079	0	∞	−1.5	1.59	5.01	37.7	20.4

in the steel brad.

air to 2.0 with air saturated solution.

Alkaline cyanide solution. Excellent results were achieved with the alkaline cyanide solution; the copper content in the scrap was reduced to less than 0.06%. This is a level which has not been attained by any physical separation method other than strenuous hand picking. Power consumption is low; it ranges from −0.01 W·h/g (no power is needed for the electrolysis) of copper removed at a cell current of 20 mA to 0.49 W·h/g of copper removed at 200 mA. Only one Faraday of electricity is needed to dissolve 1 gram-mole of copper as indicated in column (13). This implies that the cuprous cyanide complex is the dissolution product. The main drawback of this system is that no copper was deposited at the carbon cathode because of low cuprous cyanide concentrations. Addition of cuprous cyanide to the electrolyte results in copper deposition at the cathode; however, it also retards the corrosion of copper at the anode. It appears that the ratio of free cyanide-to-copper content in the electrolyte is an important factor in the overall performance. Further effort is required to determine the optimal ratio for scrap treatment. This preliminary study has, nevertheless, demonstrated that it is technologically feasible to remove copper from scrap steel with a packed-bed electrochemical cell.

ACKNOWLEDGMENT

The author wishes to thank John McWatters, Electrochemistry Department, General Motors Research Laboratories, for his help in construction of the packed-bed electrochemical cell, and the Analytical Chemistry Department, General Motors Research Laboratories, who performed the chemical analyses for this study.

LITERATURE CITED

Albrecht, O. W., and R. G. McDermott, "Economic and Technological Impediment to Recycling Obsolete Ferrous Solid Waste," *U.S. Environmental Protection Agency Rept. No. EPA-670/5-73-021* (1973).

Battelle Memorial Institute, "Measurement and Improvement of Scrap Quality," Institute of Scrap Iron and Steel, Washington D.C. (1960).

Bureau of Mines, "Automobile Disposal, A National Problem," *U.S. Bureau of Mines Special Publication No. 1-67*, U.S. Department of Interior, Washington D.C. (1967).

Chin, D-T., "Anodic Mechanism of Electrochemical Machining: Study of Current Transient on a Rotating Electrode," *J. Electrochem. Soc.*, **119**, 174 (1971).

———, "Anodic Films in ECM Electrolytes: Onset of Passivation of Mild Steel in Nitrate Solution," *ibid.*, 1181 (1972).

———, "Dissolution of Mild Steel with a Rotating Ring-Hemispherical Electrode," *ibid.*, **121**, 1592 (1974).

Institute of Scrap Iron and Steel, Inc., "Identification of Opportunities for Increased Recycling of Ferrous Solid Waste," *U.S. Environmental Protection Agency Rept. No. EPA-SW-45D-72* (1972).

Oden, L. I., A. Adams, and A. D. Fugate, "Reducing Copper and Tin Impurities in Ferrous Scrap Recovered from Incinerated Municipal Refuse," *Bureau of Mines Rept. of Investigations 7776* (1973).

Pourbaix, M., *Atlas of Electrochemical Equilibria in Aqueous Solutions*, Pergamon Press, New York (1966).

Manuscript received November 12, 1976; revision received March 17, and accepted March 30, 1977.

Combustion Kinetics in the Modeling of Large, Pulverized Fuel Furnaces: A Numerical Experiment in Sensitivity

ALLEN LOWE
TERRY F. WALL
and
IAN McC. STEWART
Department of Chemical Engineering
The University of Newcastle
N.S.W. Australia

A mathematical model of combustion in a utility type of pulverized, coal fired furnace is developed by dividing the furnace into a number of isothermal zones. The method dovetails the combustion rate data available for single char particles with a gas flow pattern to predict local combustion heat release rates and local radiation absorption coefficients, which are used as input to a zoned heat transfer model.

The furnace heat transfer is shown to be insensitive to combustion related parameters such as coal rank and coal fineness. For carbon in ash, local gas temperature, and to a lesser extent local heat flux, significant variations are predicted. It is concluded that for calculation of radiative heat transfer, combustion data are adequate. Further research activity on ignition and combustion stability, together with the radiative properties of fly ash, is recommended.

SCOPE

Despite the introduction of nuclear power stations and the active research into alternative energy sources, the bulk of electricity generated throughout the world uses conventional water tube boilers burning fossil hydrocarbons as a primary energy source. A large proportion of these boilers burn coal in a pulverized form, and with the increasing restrictions on availability of oil and natural gas, this proportion will surely increase.

Coal fired steam cycles usually operate on the Rankine cycle, most often with superheat and reheat. At present, this cycle has a maximum thermal efficiency of about 40%. This is limited mainly by the temperature to which the

---

Correspondence concerning this paper should be addressed to Terry F. Wall.